Sustainable Synthesis of Copper Oxide and Manganese Oxide Nanoparticles Using *Moullava spicata* (Dalzell ex Wight) Nicolson Leaf Extract: Characterization and Functional Applications

Priyanka R Kokate and Manohar V Lokhande*
PG-Research Centre, Department of Chemistry, Sathaye College (Autonomous), Mumbai-400057, Maharashtra, India
https://orcid.org/0009-0001-4561-1898 and https://orcid.org/0000-0002-7521-1262

ABSTRACT

As sustainable nanotechnology focuses on eco-friendly methods for creating nanoparticles, researchers have made progress in developing sustainable methods to synthesise them. The present investigation highlights the potential of *Moullava spicata* (Dalzell ex Wight) Nicolson as both a natural reducing and stabilising agent to successfully produce copper oxide (CuONPs) and manganese oxide (MnONPs) nanoparticles. The results of UV-visible spectroscopy and FTIR showed that the formation of these nanoparticles was successful due to phytochemical compounds that worked as reducing and stabilising agents. The XRD results demonstrated the crystalline structure and quality of MnONPs and CuONPs and the TEM images showed that the size distributions of both types of nanoparticles were below 100 nm. Elemental composition and purity were further confirmed with EDS analysis. CuONPs exhibited pronounced antibacterial efficacy, effectively inhibiting the growth of various bacterial strains, while MnONPs exhibited strong antibacterial activity only against Staphylococcus aureus and Proteus sp. The antioxidant activity of CuONPs was superior to that of the plant extract and MnONPs, based on the DPPH radical scavenging test results. Both copper oxide and manganese oxide nanoparticles facilitated their nano catalytic properties. The kinetic studies of each nanoparticle's catalysis produced a great reaction rate constant.

Keywords: Green synthesis; Copper oxide nanoparticles; Manganese oxide nanoparticles; Antibacterial activity; Antioxidant activity; Catalytic reduction; Nanobiotechnology

GRAHICAL ABSTRACT

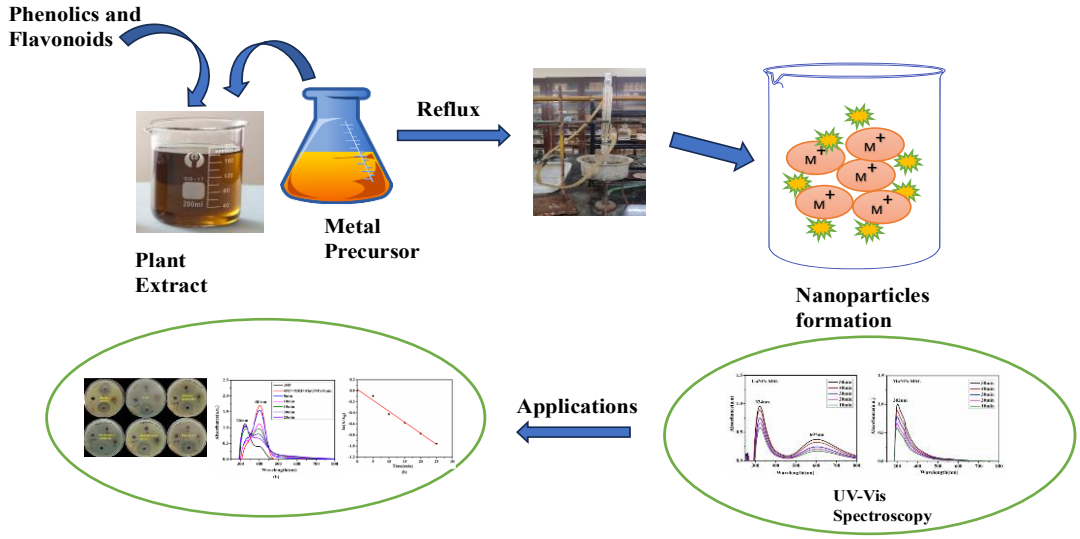

1.0 INTRODUCTION

Nanotechnology has rapidly evolved into one of the most important emerging scientific fields, thanks primarily to its many applications ranging from medicine, environmental remediation, catalysis, agriculture, electronics and biotechnology. Nanoparticles have distinctive characteristics, including increased surface-to-volume ratio, increased reactivity at different temperatures and size-dependent physicochemical behaviour, which clearly differentiate them from conventional bulk counterparts [1].

Metal oxide nanoparticles are a unique subclass of nanoparticles because they have desirable characteristics such as high levels of stability, compatibility with biological systems and multifunctionality within the industrial and medical sectors and therefore represent the most promising types of nanoparticles [2-5].

Conventional methods for synthesizing nanoparticles are typically hazardous, energy-intensive and negatively impact the environment. In contrast to traditional methods of producing nanoparticles, so-called "green" methods of synthesizing nanoparticles represent an environmentally sustainable solution to this problem [6,7]. One particularly exciting approach to green synthesizing nanoparticles is using plant materials as reducing agents (instead of harmful chemicals) because plant extracts contain many active biochemical compounds such as phenolics, flavonoids, tannins, alkaloids, terpenoids, proteins and polysaccharides. The use of plant materials to create environmentally safe nanoparticles eliminates the need for toxic chemicals while providing an inexpensive, simple and environmentally safe means of synthesizing environmentally benign nanoparticles [8-10]

CuO nanoparticles have an abundance of uniqueness, being very well known for their usefulness as an alternative form of antibacterial, antioxidant, catalyst, optical and semiconductor materials [11]. Similarly, MnO is also a popular candidate for further research. MnO exhibits its own catalytic properties, possesses a redox potential, has magnetic properties and shows tremendous promise in both environmental and biomedical applications. The biocatalytic activity and efficiency of both CuO and MnO nanoparticles are highly influenced by interconnected properties. Green synthesis has demonstrated an efficient way of tuning the properties of both CuO and MnO particles throughout biosynthesis [12-15].

Medicinal plants of great interest include *Moullava spicata* (Dalzell ex Wight) Nicolson. This plant has a wide variety of phytochemicals with research describing efficacy in phenolic compounds, flavonoids, alkaloids and other metabolites with antioxidant and antimicrobial properties. It is therefore probable that the bioactive phytochemicals present in *Moullava spicata* leaves will reduce metal ions. The resultant metal oxide nanoparticles make this species an attractive candidate for the green synthesis of metal oxide nanomaterials. To date, no research has been completed regarding the application of *Moullava spicata* leaf extracts in the biosynthesis of CuO-NPs or MnO-NPs [16-19].

CuO and MnO nanoparticles were produced in this research utilizing the eco-friendly and sustainable aqueous leaf extract of *Moullava spicata*. Numerous techniques were employed to characterise the nanoparticles. By carefully assessing the ways a certain application could work in the field of biomedicine or the environment, we performed a thorough evaluation of the antibacterial, antioxidant and catalytic action related to each type of nanoparticle. The findings discussed herein represent an added level of understanding about the potential benefits of using green-nanomaterials derived from plant sources with multiple uses [20-24].

2.0 MATERIALS AND METHODS

2.1. Chemicals and reagents: All Chemicals and reagents, which were analytical grade and employed directly without additional purification. The starting salts for the production of CuONPs and MnONPs were ($CuCl_2 \cdot 2H_2O$) Copper (II) chloride dihydrate and ($Mn(OAc)_2 \cdot 4H_2O$), Manganese (II) acetate tetrahydrate. In the catalytic reduction experiments, the reactants were p-nitrophenol and sodium borohydride ($NaBH_4$), supplied by Merck, India. To evaluate antioxidant activity, standard ascorbic acid and the radical molecule 2,2-diphenyl-1-picrylhydrazyl were procured from HiMedia Laboratories, India. Water used for preparing the aqueous solutions was double-distilled. Fresh leaf material from *Moullava spicata* (Dalzell ex Wight) Nicolson was collected and used as the biological source for creating the nanoparticles.

2.2 Methodology

2.2.1 Preparation of Leaf Extract: *Moullava spicata* (Dalzell ex Wight) Nicolson was prepared for the extraction of phytochemicals from fresh leaves, which were rinsed with distilled water to eliminate surface contaminants and residual impurities, dried in the shade and then cut into small pieces. The processed leaves were boiled in double-distilled water for 30 minutes to facilitate the extraction of phytochemical constituents. After the extract had cooled. It was then filtered through

Whatman filter paper to separate the solid particles from the aqueous extract. The clear aqueous extract was kept at 4°C until required for the biosynthesis of CuONPs and MnONPs.

2.2.2 Synthesis of CuONPs and MnONPs: The metal ions were taken up in separate, aqueous solutions of copper (II) chloride dihydrate ($CuCl_2 \cdot 2H_2O$) and manganese acetate tetrahydrate ($Mn(OAc)_2 \cdot 4H_2O$), which were mixed with the leaf extract. Following this mixing step, mixtures were heated by refluxing for 2 hours at 80 °C, to produce nanoparticles as evidenced by a colour change, after the reaction was complete. The precipitated products were collected, then centrifuged at 5000 rpm and dried in a hot air oven. After that, the materials were calcined at 500°C for 3 hours to produce both crystalline CuONPs and MnONPs.

2.3 Preliminary Phytochemical Screening of *Moullava spicata* Leaf Extract: It was confirmed through phytochemical analysis on the aqueous extract of the leaf of *Moullava Spicata* that there were several active constituents present. The metabolites detected in this study include flavonoids, tannins, phenolic compounds, proteins, saponins and alkaloids. However, terpenoids were not detected. These results suggest that the presence of these metabolites in leaf extract has a wide variety of secondary metabolites that can aid in the formation of nanoparticles. Flavonoids and phenolic constituents function as potent reducing agents, whereas proteins, tannins, saponins and alkaloids play a role in capping and stabilisation [25, 26].

2.4 Physicochemical Characterization of CuONPs and MnONPs: A variety of analytical techniques were used to assess the structural, optical, morphological, elemental and functional characteristics. Nanoparticle formation and optical properties were determined by UV-Vis spectroscopy; FTIR spectroscopy was used to determine the functional groups attributed to both reducing and stabilizing the nanoparticles. The XRD analysis provided information about the crystalline phase and associated structural attributes. Evaluation of surface morphology of the nanoparticles, as well as size determination, was accomplished using TEM, while elemental composition was determined using EDX techniques [27, 28]. By combining these techniques, a complete understanding of the physicochemical properties of the nanoparticles was generated.

3.0 RESULTS AND DISCUSSION

3.1 UV–Visible Spectrophotometry

3.1.1 *Moullava spicata* Leaf Extract: A peak at 256 nm (Figure 1a) derived from the UV-Vis measurement of an aqueous solution extracted from the leaves of *Moullava spicata*, indicates phenolic, flavonoid and other similar compounds with a conjugated system of pi-electrons from the plant extract. These plant materials can act as reducing metal ions to their respective metal oxide nanoparticle forms, as well as to inhibit or prevent the agglomeration of such nanoparticles through capping. Therefore, the results of the UV-Vis spectral analysis indicate that leaf extract is suitable for green synthesis of nanoparticles [29, 30].

3.1.2 CuONPs: The existence of CuO NPs was confirmed through UV-vis spectroscopy within the range of 200-800 nm. Qualitative analysis of CuO NPs showed (Figure 1b) two clear peaks at 324 nm and 607 nm within the spectrum. The spectrum changed over time, as evidenced by the reduction of the copper ions and formation of CuO NPs. The peak at 324 nm indicates interbond charge transfer, whereas the broad peak at 607 nm suggests the occurrence of surface plasmon resonance [31, 32]. Therefore, it is concluded that CuO NPs were created from reduced copper ions.

3.1.3 MnONPs: Manganese oxide nanoparticles (MnONPs) were confirmed by observing an absorption peak at approximately 302 nm over time, specifically 10 - 50 min (Figure 1c). This peak shows the SPR of MnONPs and evidence that manganese ions were reduced by phytochemical compounds found in *Moullava spicata* leaf extract. The single absorption peak shape indicates that uniform nanoparticles were made. The absence of any other absorption bands indicates high purity of the MnO nanoparticles, with little or no aggregates or secondary phases. Given these results, it can be concluded that high-quality MnO nanoparticles were produced [33, 34].

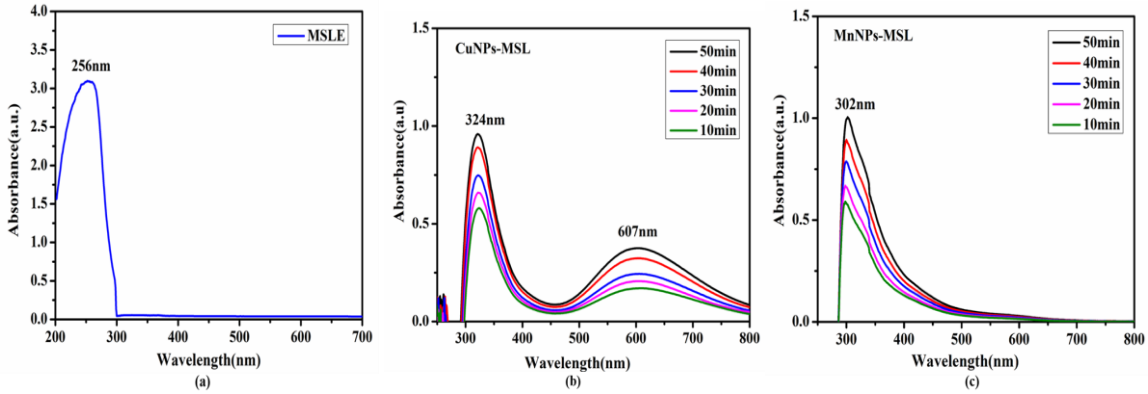

Figure 1: UV-VIS absorption spectra of synthesised (a)MSLE, (b)CuNPs and(c)MnNPs

3.2 FTIR Analysis

3.3.1 *Moullava spicata* Leaf Extract: The *Moullava spicata* leaf-based aqueous extract successfully identified a variety of functional groups. There were characteristic absorption bands corresponding to the functional groups detected at 3279.57cm^{-1}, 1549.80cm^{-1}, 1375.24cm^{-1} and 1070.88 cm^{-1}. The broad absorption band detected at 3279.57 cm^{-1} was observed to correspond to O–H stretching vibrations of hydroxyl groups. The 1549.80 cm^{-1} peak corresponds to either an N-H bending (amide) or an aromatic C=C (double bond) stretching, while the peaks at both 1375.24 cm^{-1} and 1070.88 such as C-H bending (aliphatic) and C-O stretching, respectively, (Figure 2a) were also present [35,36]. The data suggest that phytochemicals such as flavonoids, phenolics and proteins may be present in the extract, which is utilised to reduce metal ions and stabilise nanoparticles in green synthesis.

3.3.2 CuONPs: The synthesized copper oxide nanoparticles' FTIR spectrum has multiple unique bands, shown Figure 2b, including 3745.89 cm^{-1}, 3646.92 cm^{-1}, 1051.27 cm^{-1}, 471.52 cm^{-1}, 442.93 cm^{-1} and 403.06 cm $^{-1}$. The bands around 3745.89 cm^{-1} and 3646.92 cm^{-1} correspond to O–H stretching vibrations, indicating biomolecules containing hydroxyl groups on the surface of CuONP. The band around 1051.27 cm^{-1} corresponds to C–O stretching and suggests that phenolic and alcoholic groups are participating in the stabilization of CuONPs. The bands around 471.52 cm^{-1}, 442.93 cm^{-1} and 403.06 cm^{-1} were confirmed to be the result of Cu–O stretching vibrations, indicating that copper oxide nanoparticles were indeed formed [37].

3.3.3 MnONPs: MnO nanoparticles showed Figure 2c absorption bands at 1034.39cm^{-1}, 600.25cm^{-1}, 471.28cm^{-1} and 417.13 cm^{-1}. The absorption band at 1034.39 cm^{-1} indicates C-O stretching vibrations, which indicates that there are phytochemicals present on the surface of nanoparticles, from the *Moullava spicata* leaf extract. The peak at 600.25 cm^{-1} and the peaks at 471.28 cm^{-1} and 417.13 cm^{-1} correspond to Mn-O stretching vibrations, which would indicate that manganese oxides have formed in the nanoparticles [38, 39].

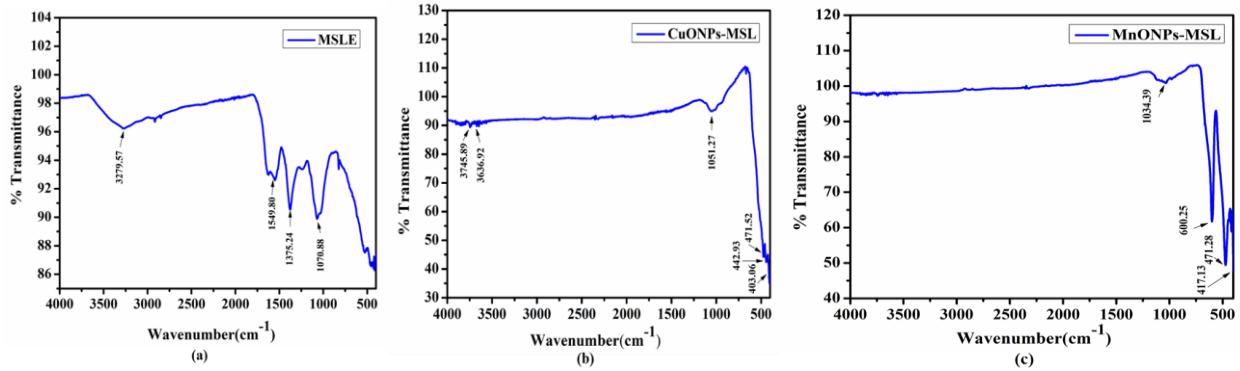

Figure 2: FTIR spectra of synthesised (a)MSLE (b)CuONPs and(c)MnONPs

3.3 XRD Analysis

3.3.1. CuONPs: The synthesized CuONPs were evaluated for both crystallinity and phase purity through analysis performed via X-ray diffraction (XRD). Diffraction patterns display Table 1, numerous characteristic peaks located at angles defined by 2θ = 32.59°, 35.63°, 38.74°, 48.85°, 53.54°, 58.24°, 61.61°, 66.33°, 68.15°, 71.92° and 75.01°, corresponding to the (110), (−111), (111),

(−202), (020), (202), (−113), (311), (220), (−311) and (004) planes, respectively. which represent the crystallographic planes of monoclinic CuO [40]. As these reflections were present in the characteristic pattern provided on the JCPDS card no. 48-1548, it can be concluded that phase-pure CuONPs were synthesized. The highly defined, sharp and well-defined nature of the peaks is indicative of high-quality crystallinity and the absence of additional reflections confirms that there are no detectable impurities present in the material Figure 3a. An average crystallite size using the Debye-Scherrer Equation estimated the crystallite size of the synthesized CuONPs to the range of 15–46 nm, thereby confirming their nanocrystalline nature [41, 42].

Table 1: Peak indexing from d-spacing for CuONPs using MSLE

Sr. No.	Peak position (2θ°)	FWHM (2θ°)	*hkl*	d-spacing (Å)	Crystallite Size (nm)
1	32.59348	0.1869	(110)	2.74506	46.25
2	35.63264	0.2920	(−111)	2.51758	29.84
3	38.74149	0.3683	(111)	2.32241	23.88
4	48.85780	0.3209	(−202)	1.86258	28.40
5	53.54081	0.4342	(020)	1.71019	21.40
6	58.24005	0.4368	(202)	1.58289	21.74
7	61.61782	0.3328	(−113)	1.50397	29.03
8	66.33440	0.3107	(311)	1.40800	31.90
9	68.15512	0.5352	(220)	1.37476	18.72
10	71.92827	0.4326	(−311)	1.31164	23.70
11	75.01557	0.6860	(004)	1.26513	15.25

3.3.2. MnONPs: X-ray diffraction analysis confirmed their crystalline nature, as evidenced by distinct diffraction peaks observed at characteristic 2θ positions of 18.10°, 29.02°, 31.12°, 32.45°, 36.21°, 38.16°, 44.54°, 50.86°, 53.95°, 56.10°, 58.59°, 59.98°, 64.76° and 69.82° corresponding to crystallographic planes (111), (200), (210), (211), (220), (221), (310), (311), (222), (400), (331), (420), (422) and (511) respectively (Table 2). The XRD pattern of Mn_3O_4 matched well with standard card No. 24-0734 for tetragonal hausmannite, thus confirming successful phase formation. D-spacing values calculated were consistent with indexed planes and the Debye–Scherrer analysis estimated the average crystallite dimension to be around 29 nm with a range between 22.27 nm and 40.66 nm, validating the synthesized MnONPs as having a nanocrystalline nature and high phase purity shown in Figure 3b [43, 44].

Table 2: Peak indexing from d-spacing for MnONPs using MSLE

Sr. No.	Peak position (2θ°)	FWHM (2θ°)	*hkl*	d-spacing (Å)	Crystallite Size (nm)
1	18.10396	0.2388	(111)	4.89604	35.18
2	29.02409	0.2539	(200)	3.07401	33.75
3	31.12026	0.2998	(210)	2.87157	28.73
4	32.44900	0.2986	(211)	2.75695	28.94
5	36.20946	0.2924	(220)	2.47879	29.86
6	38.16038	0.3942	(221)	2.35643	22.27
7	44.54041	0.3343	(310)	2.03258	26.82
8	50.85502	0.3856	(311)	1.79402	23.82
9	53.94514	0.3475	(222)	1.69832	26.79
10	56.09612	0.2312	(400)	1.63819	40.66
11	58.59030	0.3488	(331)	1.57425	27.27
12	59.98322	0.3767	(420)	1.54098	25.43
13	64.75627	0.3423	(422)	1.43845	28.70
14	69.81644	0.4496	(511)	1.34605	22.50

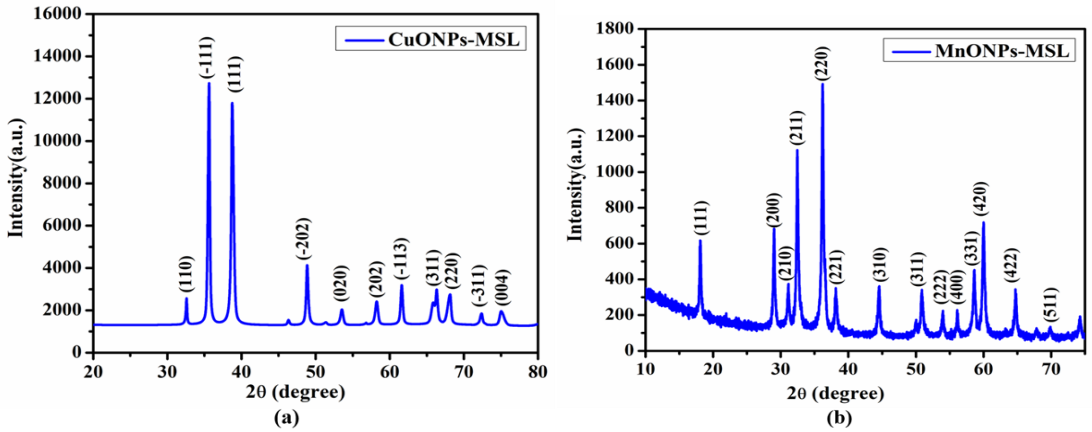

Figure 3: XRD spectrum of synthesised (a)CuONPs and (b)MnONPs

3.4 TEM Analysis

3.4.1. CuONPs: Transmission electron microscopy (TEM) was employed to investigate the morphology and particle size of the synthesized copper oxide nanoparticles. Copper oxide nanoparticles exhibited rounded or "quasi-spherical" (Figure 4a) morphology with similar size distribution and negligible agglomeration. Both the size distribution and morphology of these copper oxide nanoparticles indicate that they were produced at the nanoscale level, with an average size range between 29 - 63 nm (~ 46.6 nm) [45]. The relatively uniform size distribution indicates controlled manufacture and suggests that their production can be linked to the physical and chemical stabilization and capping characteristics associated with their synthesis.

3.4.2. MnONPs: The TEM imaging results show that MnONPs were produced predominantly as spheres, with a few irregular shapes. In these images (Figure 4b), the MnONPs are seen to be uniformly dispersed within the micrograph with occasional agglomeration of small numbers of particles. The dimensions of the MnONPs are in the range of approximately 10 -35 nm (average of ~21.6 nm), which would indicate that they are nanocrystals [46]. The fact that there is a narrow range for the MnONPs particle size indicates that controlled nucleation and growth have occurred during preparation of the MnONPs; this is believed to have been aided by phytochemicals from the leaf extract of Moullava spicata acting as surfactants or stabilizers. Thus, based on the TEM imaging results, it can be concluded that MnONPs were produced with clear morphological definition, nanoscopic dimensions and a single particle size distribution.

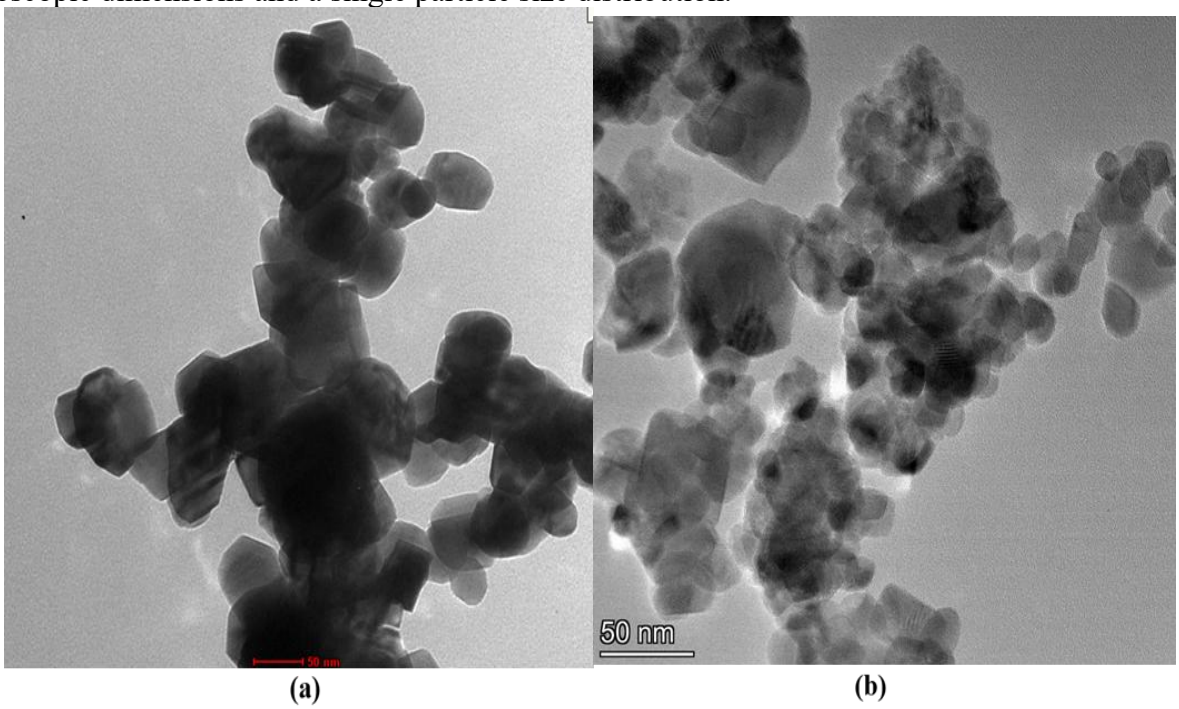

Figure 4: TEM micrograph of 50nm corresponds to (a)CuONPs and (b)MnONPs

3.5 Energy-Dispersive X-ray Spectroscopy (EDX) Analysis

3.5.1. CuONPs: The synthesized CuONPs were analyzed for elemental compositions using energy dispersive X-ray spectroscopy (EDX). From the spectra obtained, the major elements present within the CuONPs are Copper (Cu), Oxygen (O) and Carbon (C). Quantitative analysis shows that Cu represents 72.5% by weight, O 17.7% by weight and C 9.7% by weight; the corresponding atomic percentages are thus 37.3% (Cu), 36.2% (O) and 26.5% (C). The predominance of Copper and Oxygen supports the formation of copper oxide nanoparticles, as shown in Figure 5 [47, 48].

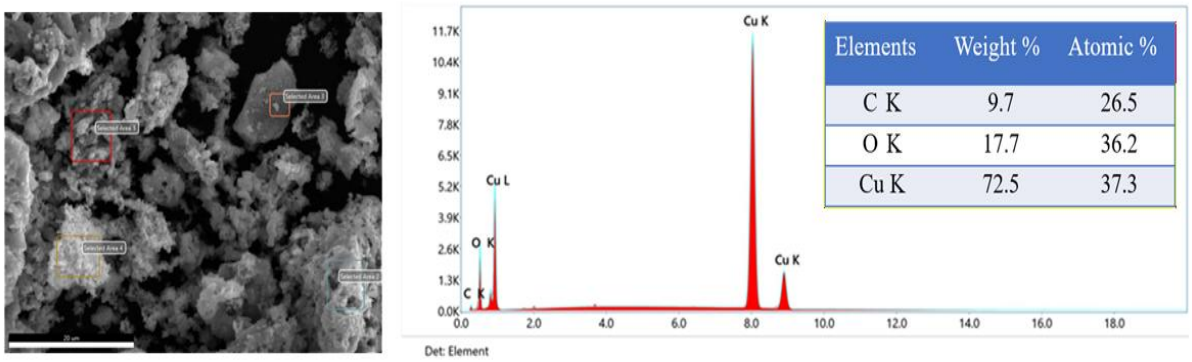

Elements	Weight %	Atomic %
C K	9.7	26.5
O K	17.7	36.2
Cu K	72.5	37.3

Figure 5: EDX spectrum of synthesised CuONPs

3.5.2 MnONPs: Energy-dispersive X-ray spectroscopy (EDX) was employed to characterize the elemental composition of the synthesized manganese oxide nanoparticles. The spectra show (Figure 6) that manganese (Mn) and oxygen (O) are the two most abundant elements, with weight percentages of 75.4% and 21.8%, respectively and atomic percentages of manganese (49.1%) and oxygen (48.7%), thus confirming that manganese oxide nanoparticles were produced. In addition to manganese and oxygen, small amounts of phosphorus (P), potassium (K) and calcium (Ca) were detected, all of which represent <0.5%, probably from residual phytochemicals [49, 50].

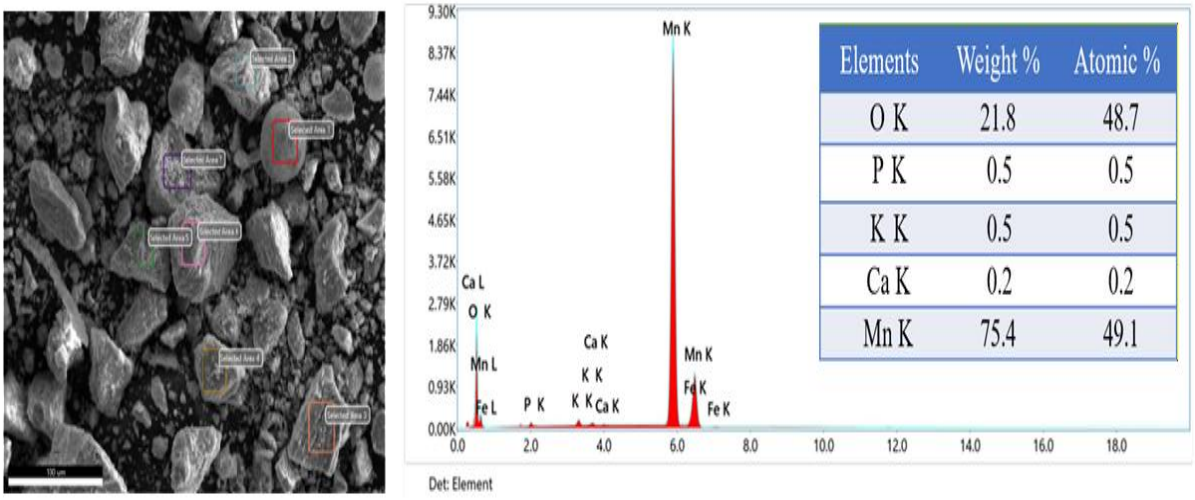

Elements	Weight %	Atomic %
O K	21.8	48.7
P K	0.5	0.5
K K	0.5	0.5
Ca K	0.2	0.2
Mn K	75.4	49.1

Figure 6: EDX spectrum of synthesised MnONPs

4.0. Antibacterial Activity: The biosynthesised copper oxide and manganese oxide nanoparticles were assessed through the agar well diffusion assay against selected bacterial strains. The CuONPs were noted against Bacillus subtilis (26.0±0.03 mm), Escherichia coli (18.0±0.03 mm), Proteus sp. (16.0±0.03 mm), Klebsiella pneumoniae (12.0±0.03 mm) and Staphylococcus aureus (12.0±0.03 mm) and no effect was found toward Pseudomonas aeruginosa. Conversely, strong antibacterial effects of the MnONPs were recorded against Staphylococcus aureus (28.0±0.03 mm), Proteus sp. (26.0±0.03 mm) and Escherichia coli (20.0±0.03 mm), while no effect was recorded toward Bacillus subtilis, Klebsiella pneumoniae and Pseudomonas aeruginosa see in Table 3, Figure 7. The inhibition zones created by CuONPs and MnONPs were all smaller than that of the positive control, streptomycin (30–34 mm); however, these data indicate that CuONPs and MnONPs exhibit good antibacterial activity [51-53].

Table 3: Antibacterial activity of CuONPs and MnONPs of MSLE

Bacterial Strain	Gram Classification	Inhibition Zone (mm): CuONPs	Inhibition Zone (mm): MnONPs	Inhibition Zone (mm): Streptomycin (+Ve Control)
Escherichia coli	Gram-negative	18± 0.03	20± 0.03	32± 0.03
Pseudomonas aeruginosa	Gram-negative	-	-	32± 0.03
Klebsiella pneumoniae	Gram-negative	12± 0.03	-	30± 0.03
Proteus sp.	Gram-negative	16± 0.03	26± 0.03	34± 0.03
Bacillus subtilis	Gram-positive	26± 0.03	-	32± 0.03
Staphylococcus aureus	Gram-positive	12± 0.03	28± 0.03	34± 0.03

Note: Values are expressed as mean zone of inhibition (mm) ± SD. Streptomycin served as the positive control. "—" indicates no significant activity.

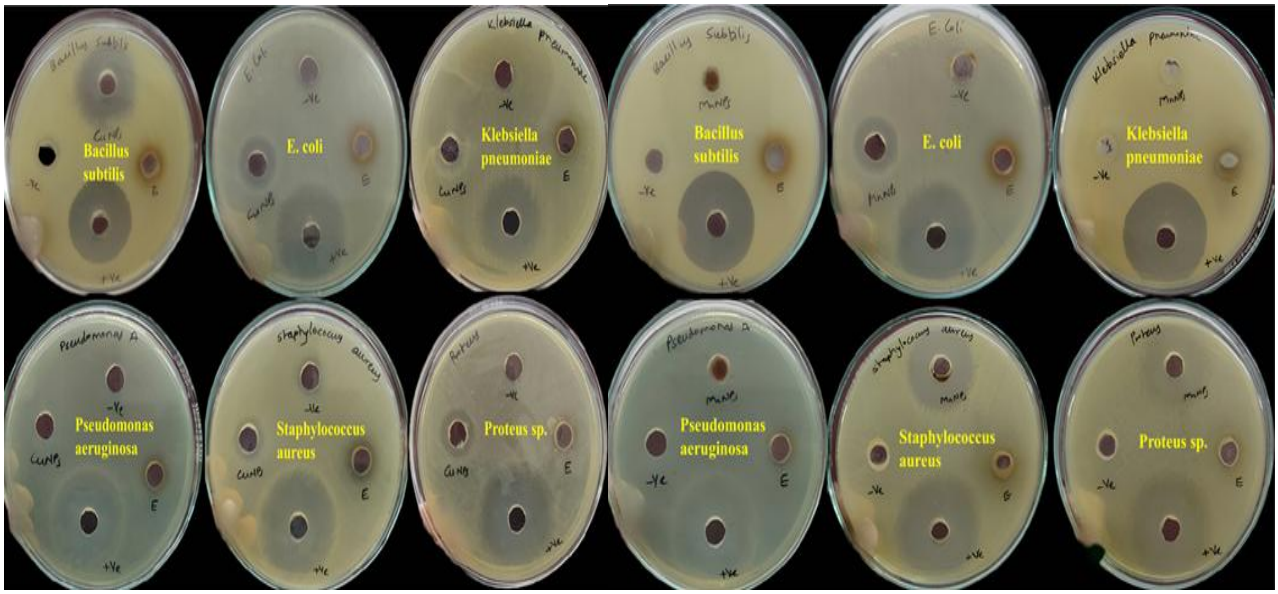

Figure 7: Antimicrobial activity of (a) CuONPs and (b) MnONPs against different microbial strains: -Ve Control: Distilled water, +Ve Control: Antibiotic, E: *Moullava spicata* leaf extract

5.0. Antioxidant Activity: Using the DPPH radical scavenging method, we evaluated the antioxidant ability of *Moullava spicata* (MSL) leaf extract, CuONPs and MnONPs and compared these results with the standard reference ascorbic acid (AA). Antioxidant activity was determined to be concentration dependent for each sample by measuring inhibition percentage from 50 µg/ml to 150 µg/ml. The highest level of radical scavenging activity among the nanoparticles was CuONPs inhibition range of 85.79 +/- 1.4 to 91.74 +/- 1.4; the next highest was MSL inhibition range of 71.82 +/- 1.4 to 80.37 +/- 1.5 and lastly, MnONPs showed the least amount of activity inhibition range of 62.92 +/- 1.5 to 72.66 +/- 1.5. As expected, ascorbic acid was found to have the strongest antioxidant activity inhibition range of 93.48 +/- 0.9 to 96.35 +/- 0.9. The calculated IC_{50} values of the samples were 29.14 µg/ml, 34.81 µg/ml, 39.73 µg/ml and 26.74 µg/ml for CuONPs, MSL, MnONPs and AA, respectively shown in Table 4. The superior antioxidant activity of CuONPs may be due to their larger surface area as well as the bonding of bioactive phytochemicals to these surfaces. These results show that CuONPs synthesized through a biological process can be utilized as agents that scavenge free radicals [54-57].

Table 4: Different Concentrations of MSL Extract, CuONPs and MnNPs Showed DPPH Free Radical Scavenging Activity

Samples	% Inhibition (Mean ± SD)					IC_{50} (µg/mL)
	50(µg/mL)	**75(µg/mL)**	**100(µg/mL)**	**125(µg/mL)**	**150(µg/mL)**	
MSL	71.82 ± 1.4	72.20 ± 1.6	75.22 ± 1.3	79.87 ± 1.7	80.37 ± 1.5	34.81
CuONPs	85.79 ± 1.4	86.73 ± 1.6	88.22 ± 1.3	89.58 ± 1.5	91.74 ± 1.4	29.14
MnONPs	62.92 ± 1.5	64.68 ± 1.7	65.22 ± 1.4	68.47 ± 1.6	72.66 ± 1.5	39.73
AA Std.	93.48 ± 0.9	93.96 ± 0.7	94.91 ± 0.8	95.08 ± 0.6	96.35 ± 0.9	26.74

Note: Values are expressed as mean ± SD (n = 3). IC_{50} values were calculated from DPPH radical scavenging activity curves. AA Std. = Ascorbic acid standard.

6.0. Catalytic Activity: The catalytic performance of CuONPs and MnONPs biosynthesized by one-step green synthesis was evaluated for the conversion of 4-NP to 4-AP in the presence of $NABH_4$. In the case of CuONPs, when monitored over a period of 30 min, a gradual decrease in absorbance with respect to 4-NP was recorded, from 1.1971 to 0.8685 and as the absorbance increased for 4-AP from 0.8516 to 1.3155 (Table 5). There was also a decrease in 4-NP absorbance from 1.7091 to 0.6565 and an increase in 4-AP absorbance from 0.4349 to 1.0522 associated with effective catalytic activity by MnONPs, in the same time span in 25 min (Table 6). A progressive decrease in the absorbance of 4-NP, along with an increase in the absorbance of 4-AP, provides direct evidence for successful catalytic conversion shown in Figures 8 and 9 [58-60]. The reason for the increased activity of both nanoparticles is attributed to their high surface area and there was efficient electron transfer between the $NaBH_4$ and 4-NP molecules via the surface of the nanoparticles. These results demonstrate that MnONPs have provided faster conversion than CuONPs under these experimental conditions.

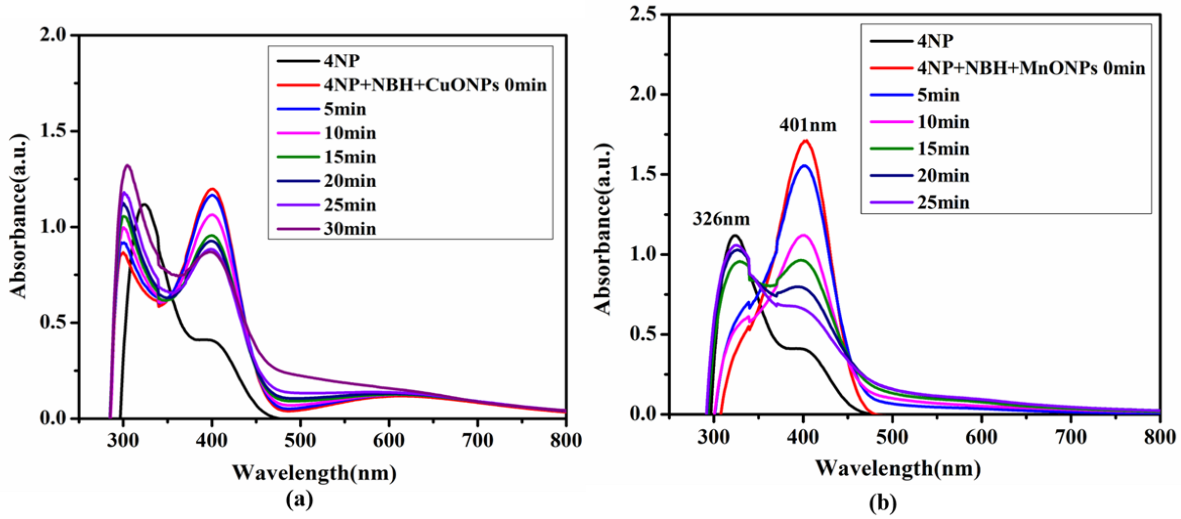

Figure 8: UV-VIS spectrum of the reduction of 4-NP by (a)CuONPs and (b) MnONPs of *Moullava spicata* leaf extract

Table 5: Catalytic Reduction of 4-NP to 4-AP by CuONP

Time (min)	Decrease in Absorbance of NP	Increase in Absorbance of AP
0	1.1971	0.8516
5	1.1663	0.912
10	1.0637	0.9858
15	0.9558	1.051
20	0.9267	1.1054
25	0.8835	1.1674
30	0.8685	1.3155

Table 6: Catalytic Reduction of 4-NP to 4-AP by MnONP

Time (min)	Decrease in Absorbance of NP	Increase in Absorbance of AP
0	1.7091	0.4349
5	1.5531	0.6175
10	1.1192	0.5602
15	0.9591	0.9541
20	0.7891	1.0252
25	0.6565	1.0525

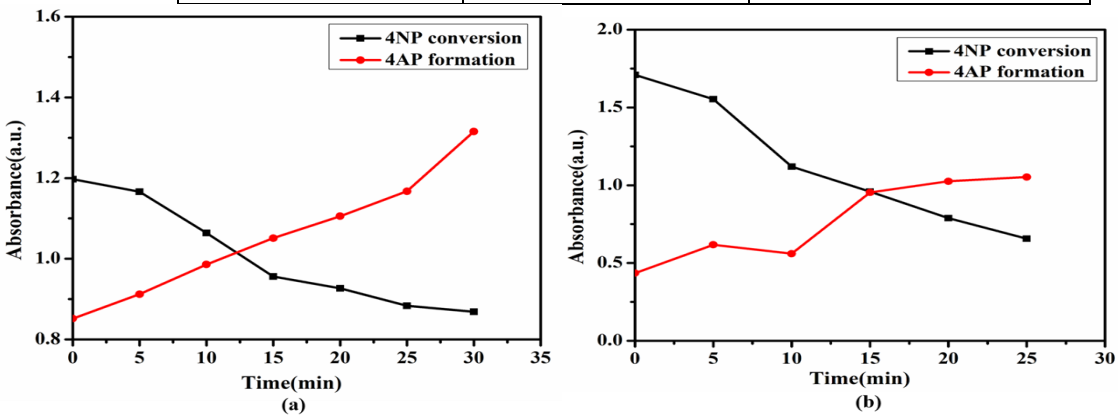

Figure 9: Conversion of 2-NP to 4-AP by using (a)CuONPs and (b)MnONPs

7.0 Kinetic study: The reduction kinetics of 4-NP were examined using a pseudo-first-order method by using a plot of $\ln(A/A_0)$ vs. time. For 4-NP reduced with CuONPs (Table 7), Linear regression analysis yielded a correlation coefficient (R^2) of 0.9422, with the corresponding rate constant calculated as $k = 0.01184\ min^{-1}$, indicating that CuONPs were efficient catalysts. MnONPs also expressed (Table 8) a linear fit, but the R^2 was determined to be 0.9851, with a rate constant of $k = 0.03984$, showing that MnONPs exhibited faster reduction rates than CuONPs in similar reaction conditions. The strong linear relationship displayed by both sets of data provides strong evidence that both reactions followed pseudo-first-order kinetics, as shown in Figure 10. Overall, both CuONPs and MnONPs are suitable catalysts for the conversion of 4-NP to 4-aminophenol, with MnONPs being more efficient [61, 62].

Table 7: Kinetic Reduction of 4-Nitrophenol Using CuONPs

Time (min)	Absorbance (A)	A/A_0	$\ln(A/A_0)$
0	1.1971	1.0000	0.0000
5	1.1663	0.9743	−0.0261
10	1.0637	0.8886	−0.1183
15	0.9558	0.7985	−0.2253
20	0.9267	0.7742	−0.2561
25	0.8835	0.7377	−0.3042
30	0.8685	0.7256	−0.3211

Table 8: Kinetic Reduction of 4-Nitrophenol Using MnONPs

Time (min)	Absorbance (A)	A/A_0	$\ln(A/A_0)$
0	1.7091	1.0000	0.0000
5	1.5531	0.9087	−0.0957
10	1.1192	0.6548	−0.4237
15	0.9591	0.5613	−0.5779
20	0.7891	0.4617	−0.7731
25	0.6565	0.3842	−0.9570

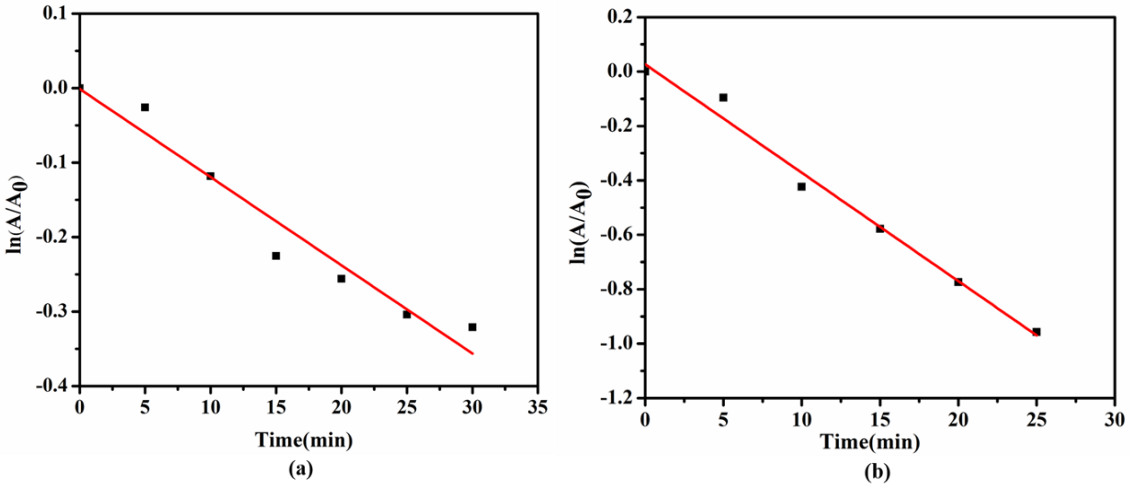

Figure 10: linear relationship between $\ln(A/A_0)$ vs. reaction time (a)CuONPs and (b)MnONPs

CONCLUSION

Using the aqueous leaf extract of *Moullava spicata* (Dalzell ex Wight) Nicolson, this study successfully created copper oxide nanoparticles (CuONPs) and manganese oxide nanoparticles (MnONPs) in an environmentally friendly way. The bioactive components detected during the phytochemical screening of *Moullava spicata* included phenolic compounds, flavonoids, tannins, proteins, saponins and alkaloids. The characterization techniques UV–Vis, FTIR, XRD, TEM and EDS established the nanoparticles' size, crystallinity and purity. The size distributions of CuONPs (15–46 nm) and MnONPs (22–41 nm) were verified by TEM. The biological and catalytic capabilities of the biosynthesized nanoparticles were considerable. For example, CuONPs exhibited excellent antioxidant and antibacterial activities against various pathogenic bacterial strains. Similarly, MnONPs displayed excellent antibacterial properties against Staphylococcus aureus, as well as Proteus sp. In terms of catalysis, both nanoparticles catalysed the transformation of 4-nitrophenol into 4-aminophenol, with kinetic analyses confirming that the reaction proceeded via pseudo-first-order behaviour. Moreover, MnONPs had a higher catalytic rate constant than CuONPs, thus being more efficient in reducing 4-nitrophenol.

Overall, the results suggest that the leaves of the plant, *Moullava spicata,* can be used as a sustainable source for creating nanoparticles. The CuO nanoparticles and MnO nanoparticles created through this method have many possible uses, including cleaning up the environment, making products effective against microbes and serving as ingredients in food and cosmetic products. The results demonstrate the growing interest in sustainable materials for creating new types of nanomaterials.

Competing Interests: The authors affirm that no financial interests or personal relationships exist that could have affected the research or its outcomes.

Consent for publication: Not applicable

Ethics approval and consent to participate: Not applicable

Funding: The research received no funding

ACKNOWLEDGEMENTS

The authors gratefully acknowledge the Management of PTVA, the Principal and the Head of the Department of Chemistry, Sathaye College (Autonomous), Mumbai, for providing access to laboratory facilities and instrumentation. We also extend our sincere thanks to the Central Instrumentation Facility, the Head of the Department of Botany at Sathaye College (Autonomous) and Icon Lab, Navi Mumbai, for their valuable support in TEM and XRD analyses. In addition, we wish to recognize the contributions of our colleagues and technical staff, whose assistance was indispensable throughout both the experimental and analytical phases of this research.

REFERENCES

[1] Joudeh, N., & Linke, D. (2022). Nanoparticle classification, physicochemical properties, characterization, and applications: A comprehensive review for biologists. *Journal of Nanobiotechnology*, 20, 262.DOI: 10.1186/s12951-022-01477-8

[2] Negrescu, A. M., Killian, M. S., Raghu, S. N. V., Schmuki, P., Mazare, A., & Cimpean, A. (2022). Metal oxide nanoparticles: Review of synthesis, characterization and biological effects. *Journal of Functional Biomaterials*, 13(4), 274.DOI: 10.3390/jfb13040274

[3] Stankic, S., Suman, S., Haque, F., & Vidic, J. (2016). Pure and multi metal oxide nanoparticles: Synthesis, antibacterial and cytotoxic properties. *Journal of Nanobiotechnology*, 14, 73. DOI: 10.1186/s12951-016-0225-6

[4] Gebre, S. H., & Sendeku, M. G. (2019). New frontiers in the biosynthesis of metal oxide nanoparticles and their environmental applications: An overview. *SN Applied Sciences*, 1, 928. DOI: 10.1007/s42452-019-0931-4

[5] Xu, L. (2018). Stability and reactivity: Positive and negative aspects for nanoparticle processing. *Chemical Reviews*, 118(7), 3209–3250.DOI: 10.1021/acs.chemrev.7b00208

[6] Iravani, S. (2011). Green synthesis of metal nanoparticles using plants. *Green Chemistry*, 13(10), 2638–2650.DOI: 10.1039/C1GC15386B

[7] Ahmed, S., Ahmad, M., Swami, B. L., & Ikram, S. (2016). A review on plants extract mediated synthesis of silver nanoparticles for antimicrobial applications: A green expertise. *Journal of Advanced Research*, 7(1), 17–28.DOI: 10.1016/j.jare.2015.02.007

[8] Mittal, A. K., Chisti, Y., & Banerjee, U. C. (2013). Synthesis of metallic nanoparticles using plant extracts. *Biotechnology Advances*, 31(2), 346–356.DOI: 10.1016/j.biotechadv.2013.01.003

[9] Khalil, A. T., Ovais, M., Ullah, I., Ali, M., Shinwari, Z. K., & Maaza, M. (2018). Biosynthesis of metal nanoparticles via biological entities and their applications. *Applied Microbiology and Biotechnology*, 102(16), 6799–6813.DOI: 10.1007/s00253-018-9148-5

[10] Singh, P., Kim, Y. J., Zhang, D., & Yang, D. C. (2016). Biological synthesis of nanoparticles from plants and microorganisms. *Trends in Biotechnology*, 34(7), 588–599. DOI: 10.1016/j.tibtech.2016.02.006

[11] Ren, G., Hu, D., Cheng, E. W. C., Vargas-Reus, M. A., Reip, P., & Allaker, R. P. (2009). Characterisation of copper oxide nanoparticles for antimicrobial applications. *International Journal of Antimicrobial Agents*, 33(6), 587–590.DOI: 10.1016/j.ijantimicag.2008.12.004

[12] Siddiqi, K. S., ur Rahman, A., Tajuddin, & Husen, A. (2018). Properties of zinc oxide nanoparticles and their activity against microbes. (Includes comparative discussion of metal oxide nanoparticles such as CuO and MnO.) *Nanoscale Research Letters*, 13, 141. DOI: 10.1186/s11671-018-2532-3

[13] Jeevanandam, J., Barhoum, A., Chan, Y. S., Dufresne, A., & Danquah, M. K. (2018). Review on nanoparticles and nanostructured materials: History, sources, toxicity and regulations. *Beilstein Journal of Nanotechnology*, 9, 1050–1074.DOI: 10.3762/bjnano.9.98

[14] Das, R., Vecitis, C. D., Schulze, A., Cao, B., Ismail, A. F., Lu, X., Chen, J., & Ramakrishna, S. (2017). Recent advances in nanomaterials for water protection and monitoring. *Chemical Society Reviews*, 46(22), 6946–7020.DOI: 10.1039/C6CS00520E

[15] Chen, D. H., & Hsieh, C. H. (2002). Synthesis of nickel and manganese oxide nanoparticles and their catalytic applications. *Journal of Materials Chemistry*, 12(8), 2412–2415.DOI: 10.1039/B202514A

[16] Makarov, V. V., Love, A. J., Sinitsyna, O. V., Makarova, S. S., Yaminsky, I. V., Taliansky, M. E., & Kalinina, N. O. (2014). "Green" nanotechnologies: Synthesis of metal nanoparticles using plants. *Acta Naturae*, 6(1), 35–44.DOI: 10.32607/20758251-2014-6-1-35-44

[17] Saratale, R. G., Benelli, G., Kumar, G., Kim, D. S., & Saratale, G. D. (2018). Exploiting antidiabetic potential of silver nanoparticles synthesized using medicinal plants. *Artificial Cells, Nanomedicine, and Biotechnology*, 46(sup3), S708–S720.DOI: 10.1080/21691401.2018.1439830

[18] Akintelu, S. A., Folorunso, A. S., Folorunso, F. A., & Oyebamiji, A. K. (2020). Green synthesis of copper oxide nanoparticles for biomedical applications and environmental remediation. *Heliyon*, 6(7), e04508.DOI: 10.1016/j.heliyon.2020.e04508

[19] El-Naggar, N. E. A., Hussein, M. H., & Shaaban-Dessuuki, S. A. (2018). Production, characterization and applications of biosynthesized metal nanoparticles. *Scientific Reports*, 8, 1–15.DOI: 10.1038/s41598-018-19275-6

[20] Naseem, T., & Farrukh, M. A. (2015). Antibacterial activity of green synthesis of iron nanoparticles using plant extracts. *Journal of Chemistry*, Article ID 912342.DOI: 10.1155/2015/912342

[21] Gahlawat, G., Choudhury, A. R., Baskar, G., & Kumar, A. (2016). Biogenic synthesis of metal oxide nanoparticles and their applications. *RSC Advances*, 6, 6581–6594.DOI: 10.1039/C5RA23283A

[22] Khan, I., Saeed, K., & Khan, I. (2019). Nanoparticles: Properties, applications and toxicities. *Arabian Journal of Chemistry*, 12(7), 908–931.DOI: 10.1016/j.arabjc.2017.05.011

[23] Salam, H. A., Rajiv, P., Kamaraj, M., Jagadeeswaran, P., Gunalan, S., & Sivaraj, R. (2012). Plants: Green route for nanoparticle synthesis. *International Research Journal of Biological Sciences*, 1(5), 85–90.DOI: 10.13140/RG.2.1.3005.6807

[24] Vijayakumar, S., Malaikozhundan, B., Shanthi, S., & Vaseeharan, B. (2016). Green synthesis of metal nanoparticles using medicinal plants and their biological applications. *Microbial Pathogenesis*, 101, 1–11.DOI: 10.1016/j.micpath.2016.10.020

[25] Toledo, A. G., Souza, J. G. L., Santana, C. B., Mallmann, A. P., Santos, C. V., Corrêa, J. M., & Pinto, F. G. S. (2021). Antimicrobial, antioxidant activity and phytochemical prospection of *Eugenia involucrata* DC. leaf extracts. *Brazilian Journal of Biology, 83*, e245753. DOI: 10.1590/1519-6984.245753

[26] Mahendran, G., Verma, S. K., & Rahman, L. U. (2021). The traditional uses, phytochemistry and pharmacology of *Mentha spicata* L.: A review. *Journal of Ethnopharmacology, 278*, 114266.DOI: 10.1016/j.jep.2021.114266

[27] Amin, F., Khattak, B., Alotaibi, A., Qasim, M., Ahmad, I., Ullah, R., Alqahtani, A. S., & Alqahtani, M. S. (2021). Green synthesis of copper oxide nanoparticles using *Aerva javanica* leaf extract and their characterization and investigation of in vitro antimicrobial potential and cytotoxic activities. *Evidence-Based Complementary and Alternative Medicine, 2021*, 5589703.DOI: 10.1155/2021/5589703

[28] Souri, M., Hoseinpour, V., Shakeri, A., & Ghaemi, N. (2018). Optimisation of green synthesis of MnO nanoparticles via utilising response surface methodology. *IET Nanobiotechnology, 12*(6), 822–827.DOI: 10.1049/iet-nbt.2017.0145

[29] Nande, A., Raut, S., Michalska-Domanska, M., & Dhoble, S. J. (2021). Green synthesis of nanomaterials using plant extract: A review. *Current Pharmaceutical Biotechnology, 22*(13), 1794–1811.DOI: 10.2174/1389201021666201117121452

[30] Salem, S. S., & Fouda, A. (2021). Green synthesis of metallic nanoparticles and their prospective biotechnological applications: An overview. *Biological Trace Element Research, 199*(1), 344–370.DOI: 10.1007/s12011-020-02138-3

[31] Khaldari, M., Yazdani-Elah-Abadi, A., & Ahmadi, F. (2021). Eco-friendly synthesis of copper oxide nanoparticles using plant extract and evaluation of their catalytic and antibacterial activities. *RSC Advances, 11*(19), 11039–11058.DOI: 10.1039/D0RA09924D

[32] Akintelu, S. A., Folorunso, A. S., Folorunso, F. A., & Oyebamiji, A. K. (2020). Green synthesis of copper oxide nanoparticles for biomedical application and environmental remediation. *Heliyon, 6*(7), e04508.DOI: 10.1016/j.heliyon.2020.e04508

[33] Nagaraja, K., Arunpandian, M., & Hwan, O. T. (2024). A facile green synthesis of manganese oxide nanoparticles using gum karaya polymer as a bioreductant for efficient photocatalytic degradation of organic dyes and antibacterial activity. *International Journal of Biological Macromolecules, 273*, 133123.DOI: 10.1016/j.ijbiomac.2024.133123

[34] Drummer, S., Madzimbamuto, T., & Chowdhury, M. (2021). Green synthesis of transition-metal nanoparticles and their oxides: A review. *Materials, 14*(11), 2700.DOI: 10.3390/ma14112700

[35] Makarov, V. V., Love, A. J., Sinitsyna, O. V., Makarova, S. S., Yaminsky, I. V., Taliansky, M. E., & Kalinina, N. O. (2014). Green nanotechnologies: Synthesis of metal nanoparticles using plants. *Acta Naturae, 6*(1), 35–44.DOI: 10.32607/20758251-2014-6-1-35-44

[36] Bankar, A., Joshi, B., Kumar, A. R., & Zinjarde, S. (2010). Banana peel extract mediated novel route for the synthesis of silver nanoparticles. *Colloids and Surfaces A: Physicochemical and Engineering Aspects, 368*(1–3), 58–63.DOI: 10.1016/j.colsurfa.2010.07.024

[37] Ghosh, S., More, N., Nitnavare, R., Jagtap, S., Chippalkatti, R., Derle, A., Kitture, R., Kale, S., & Bellare, J. (2022). New frontiers in the plant extract mediated biosynthesis of copper oxide (CuO) nanoparticles and their potential applications: A review. *Environmental Research, 203*, 111858.DOI: 10.1016/j.envres.2021.111858

[38] Dhananjaya, N., Nagabhushana, H., Sharma, S. C., Nagaswarupa, H. P., & Vidya, Y. S. (2015). Green synthesis of MnO nanoparticles and their characterization. *Spectrochimica Acta Part A: Molecular and Biomolecular Spectroscopy*, 149, 996–1000.DOI: 10.1016/j.saa.2015.05.045

[39] Ramesh, M., Anbuvannan, M., & Viruthagiri, G. (2015). Green synthesis of MnO nanoparticles using plant extract and evaluation of their properties. *Applied Surface Science*, 349, 629–635. DOI: 10.1016/j.apsusc.2015.05.034

[40] Phiwdang, K., Suphankij, S., Mekprasart, W., & Pecharapa, W. (2013). Synthesis of CuO nanoparticles by precipitation method using different precursors. *Energy Procedia*, 34, 740–745. DOI: 10.1016/j.egypro.2013.06.808

[41] Khorsand Zak, A., Abd. Majid, W. H., Abrishami, M. E., & Yousefi, R. (2011). X-ray analysis of ZnO nanoparticles by Williamson–Hall and size–strain plot methods. *Solid State Sciences*, 13(1), 251–256.DOI: 10.1016/j.solidstatesciences.2010.11.024

[42] Wang, X., Yang, L., Chen, Z., & Shin, D. M. (2008). Application of nanotechnology in cancer therapy and imaging. *CA: A Cancer Journal for Clinicians*, 58(2), 97–110. . DOI: 10.3322/CA.2007.0003

[43] Birkner, N., & Navrotsky, A. (2014). Thermodynamics of manganese oxides: Energetics of hausmannite (Mn_3O_4) and related phases. *Proceedings of the National Academy of Sciences*, 111(17), 6209–6214.DOI: 10.1073/pnas.1404177111

[44] Thackeray, M. M. (1997). Manganese oxides for lithium batteries. *Progress in Solid State Chemistry*, 25(1–2), 1–71.DOI: 10.1016/S0079-6786(97)00004-2

[45] Nasrollahzadeh, M., Sajadi, S. M., Rostami-Vartooni, A., & Bagherzadeh, M. (2015). Green synthesis of CuO nanoparticles using plant extracts and evaluation of their catalytic activity. *Journal of Colloid and Interface Science*, 448, 106–113.DOI: 10.1016/j.jcis.2015.01.075

[46] Hong, R. Y., Pan, T. T., Qian, J. Z., & Li, H. Z. (2006). Synthesis and surface modification of Mn_3O_4 nanoparticles. *Chemical Engineering Journal*, 119(2–3), 71–81.DOI: 10.1016/j.cej.2006.03.015

[47] Rehman, F. U., Mahmood, R., Haq, S., et al. (2022). Phytogenic fabrication of copper oxide nanoparticles for antibacterial and antioxidant screening: Physico-chemical study. *Crystals*, 12(12), 1796.DOI: 10.3390/cryst12121796

[48] Mahmoud, A. E. D., Al-Qahtani, K. M., Alflaij, S. O., et al. (2021). Green copper oxide nanoparticles for lead, nickel, and cadmium removal from contaminated water. *Scientific Reports*, 11, 12547. DOI: 10.1038/s41598-021-91093-7

[49] Alhumaydhi, F. A., Aljuaid, B. S., Alharbi, N. S., et al. (2023). Green synthesis and characterization of manganese oxide nanoparticles using plant extract and evaluation of their biological activities. *Scientific Reports*, 13, 10521. DOI: 10.1038/s41598-023-37692-0

[50] Adeel, M., Saeed, M., Khan, M. S., et al. (2022). Phytofabrication of manganese oxide nanoparticles and their antimicrobial, antioxidant and catalytic applications. *Materials Chemistry and Physics*, 286, 126168.DOI: 10.1016/j.matchemphys.2022.126168

[51] Ssekatawa, K., Byarugaba, D. K., Wampande, E. M., et al. (2022). Green synthesis of copper oxide nanoparticles and their antimicrobial, antioxidant and photocatalytic activities. *Frontiers in Bioengineering and Biotechnology*, 10, 820218.DOI: 10.3389/fbioe.2022.820218

[52] Alhumaydhi, F. A., Aljuaid, B. S., Alharbi, N. S., et al. (2023). Green synthesis and biological evaluation of manganese oxide nanoparticles. *Scientific Reports*, 13, 10521. DOI: 10.1038/s41598-023-37692-0

[53] Paul, D., Pandey, A., & Neogi, S. (2023). Bacterial cell permeability study by metal oxide and mixed metal oxide nanoparticles: analysis of the factors contributing to the antibacterial activity of nanoparticles. *World Journal of Microbiology and Biotechnology*, 39, 281. DOI: 10.1007/s11274-023-03712-2

[54] Kaningini, A. G., Motlhalamme, T., More, G. K., Mohale, K. C., & Maaza, M. (2023). Antimicrobial, antioxidant, and cytotoxic properties of biosynthesized copper oxide nanoparticles (CuO-NPs) using *Athrixia phylicoides* DC. *Heliyon*, 9(4), e15265. DOI: 10.1016/j.heliyon. 2023.e15265

[55] Geremew, A., Palmer, L., Johnson, A., Reeves, S., Brooks, N., & Carson, L. (2024). Multi-functional copper oxide nanoparticles synthesized using *Lagerstroemia indica* leaf extracts and their applications. *Heliyon*, 10(9), e30178.DOI: 10.1016/j.heliyon. 2024.e30178

[56] Zaragoza, G. P., Ilem, C. N. D., Conde, B. I. C., & Garcia, J. (2024). Plant-mediated synthesis of Mn_3O_4 nanoparticles: challenges and applications. *Nanotechnology*, 35(34). DOI: 10.1088/1361-6528/ad4c71

[57] Kandasamy, S., et al. (2023). Plant-derived metal oxide nanoparticles for antioxidant and biomedical applications: recent advances. *Journal of Nanomaterials and Biomedicine*. DOI: 10.3390/nano13081368

[58] Prakruthi, R., & Deepakumari, H. N. (2024). CuO nanoparticles: green combustion synthesis, photocatalytic and catalytic applications. *RSC Advances*, 14, 28703–28715. DOI: 10.1039/D4RA04622F

[59] Kumar, K., Kumar, R., Jasrotia, R., et al. (2024). In-vitro bactericidal, antioxidant and catalytic efficacy of biosynthesized CuO/Cu_2O–NiO nanocomposites. *Discover Applied Sciences*, 6, 87. DOI: 10.1007/s42452-024-05679-7

[60] Bhatia, S., Verma, N., & Bedi, R. K. (2023). Recent advances in catalytic reduction of nitrophenols using metal oxide nanoparticles. *Catalysts*, 13(2), 298.DOI: 10.3390/catal13020298

[61] Zhang, Y., Liu, X., Wang, H., & Li, J. (2021). Catalytic reduction of 4-nitrophenol over metal oxide nanostructures: Kinetic and mechanistic insights. *Journal of Environmental Chemical Engineering*, 9(6), 106726.DOI: 10.1016/j.jece.2021.106726

[62] Sharma, P., Gupta, N., & Singh, R. (2022). Nanostructured metal oxides as efficient catalysts for reduction of nitroaromatic pollutants. *Materials Today Chemistry*, 24, 100846. DOI: 10.1016/j.mtchem.2022.100846

****